Thermal quenching of Eu2+ emission in Ca- and Sr-Ga2S4 in relation with VRBE schemes

Dobrowolska, A.P.; Dierre, Benjamin; Fang, C.M.; Hintzen, Bert; Dorenbos, Pieter

DOI
10.1016/j.jlumin.2016.12.022

Publication date
2016

Document Version
Accepted author manuscript

Published in
Journal of Luminescence

Link to formal publication in Journal of Luminescence (Elsevier): https://doi.org/10.1016/j.jlumin.2016.12.022

Thermal quenching of Eu^{2+} emission in Ca- and Sr-Ga_2S_4 in relation with VRBE schemes

A. Dobrowolska[1,2], B. Dierre[1,*], C.M. Fang[3], H.T. Hintzen[1], P. Dorenbos[1,*]

[1]Delft University of Technology, Faculty of Applied Sciences, Department of Radiation Science and Technology, Mekelweg 15, 2629JB Delft, The Netherlands

[2]Faculty of Engineering and Economics, Wrocław University of Economics, Komandorska 118/120, 53-345 Wrocław, Poland

[3]BCAST, Brunel University London, Waterside House, Cowley Business Park, Uxbridge, Middlesex, UB8 2AD. United Kingdom

*Corresponding authors: B.F.P.R.Dierre@tudelft.nl, P.Dorenbos@tudelft.nl

Abstract:

Structural and optical properties of MGa_2S_4 (M = Mg, Zn, Ca, Sr, Ba) compounds have been compared, and the vacuum referred binding energy (VRBE) schemes were constructed for the lanthanide ions in the iso-structural compounds $CaGa_2S_4$ and $SrGa_2S_4$ employing literature data. The VRBE of an electron in the 5d excited state of Eu^{2+} was found at 0.75 and 0.97 eV below the bottom of the conduction band (CB) in $CaGa_2S_4$:Eu and $SrGa_2S_4$:Eu, respectively. Such differences explains the unexpected higher thermal quenching temperature reported for Eu^{2+}-doped $SrGa_2S_4$ ($T_{50\%}$ = ~475 K) compared to Eu^{2+}-doped $CaGa_2S_4$($T_{50\%}$ = 400 K) The significantly lower VRBE at the CB-bottom in $CaGa_2S_4$ versus $SrGa_2S_4$ may be explained by the shorter Ga-S bond lengths in $SrGa_2S_4$.

Keywords: $SrGa_2S_4$; $CaGa_2S_4$; thiogallate; VRBE; thermal quenching

I Introduction

Over the past years rare-earth doped phosphors attracted more attention due to their high potential as conversion phosphors in light-emitting diodes (LEDs) for lighting or displays.[1-6] In lighting, the combination of a blue-emitting LED with yellow- or with a combination of red- and green-emitting conversion phosphors are used. Eu^{2+} has shown to be a suitable activator for realization of applicable LED phosphors.[7] Eu^{2+}-doped thiogallates, in particular $CaGa_2S_4$, $SrGa_2S_4$ and $BaGa_2S_4$, , have shown interesting luminescence properties which makes them attractive for blue-excited LED devices.[8-15] However, from an application point of view, the thermal quenching of Eu^{2+} emission in these compounds at the operation temperature of the LED chip, which can reach 150ºC (~420 K), is a major problem. Literature reports that $T_{50\%}$, defined as the temperature at which luminescence intensity drops to 50% of the initial lower temperature value, is at 400 K for Eu^{2+}-doped $CaGa_2S_4$,[16] and at ~475 K for Eu^{2+}-doped $SrGa_2S_4$ when compared with the initial intensity at room temperature.[17] Thermal quenching in Eu^{2+}-doped MGa_2S_4 was studied extensively and several thermal quenching mechanisms were proposed, like increased absorption by the host,[16] hole transfer from the Eu^{2+} 4f ground state level to the host-lattice valence band,[18, 19] or thermal activation of an electron from the 5d level of Eu^{2+} to the host-lattice conduction band.[9] Besides, it was found for Eu^{2+}-doped $SrGa_2S_4$ that thermal quenching is significantly stronger for higher Eu^{2+} concentration, which was attributed to a locally smaller energy separation between the excited 5d state and the conduction band (CB).[17] The mechanism assuming that thermal quenching proceeds via ionization by thermal excitation of an electron from the Eu^{2+} 5d state to the host-lattice CB gained a lot of acceptance over the past few years.[20] Thermally activated ionization was found to be responsible for the thermal quenching of Eu^{2+} luminescence in a number of hosts, such as $CaAl_2O_4$,[21] $GdAlO_3$,[22] $LiYP_4O_{12}$,[23] and CaS.[24] The aim of the present paper is to explain the differences in thermal quenching of Eu^{2+} emission between iso-structural $CaGa_2S_4$ and $SrGa_2S_4$ by constructing the vacuum referred binding energy (VRBE) schemes and relating this information to crystallographic structural data.

II Comparison of the properties of Eu^{2+}-doped MGa_2S_4 phosphors

Although this article will mainly focus on Eu^{2+}-doped $CaGa_2S_4$ and $SrGa_2S_4$, for sake of completeness, the structural and optical properties of the reported Eu^{2+}-doped MGa_2S_4 with M = Zn, Mg, Ca, Sr, Ba, will be first discussed. Table 1 shows a comparison of the structural and

optical properties of the different MGa_2S_4 thiogallates for similar Eu^{2+} concentration, namely the energy needed for host exciton creation (E^{ex}), determined by photoluminescence excitation spectroscopy, the Eu^{2+} emission energy (E_{fd}), the energy of the Eu^{2+} transition from the $4f^7$ ground state to the $4f^65d$ lowest excited state level (E_{df}), the energy of the zero-phonon line (E_0), the Stokes shift (ΔS) and the redshift (D) of the 4f-5d absorption, the full width at half maximum (FWHM) of the emission band at room temperature and 420 K, the temperature $T_{50\%}$ and the ratio I_{420K}/I_{RT}. MGa_2S_4 thiogallate host-lattices present different types of structures as function of M: tetragonal for $ZnGa_2S_4$,[25] monoclinic for $MgGa_2S_4$,[26] orthorhombic for $CaGa_2S_4$ and $SrGa_2S_4$,[27] and cubic for $BaGa_2S_4$.[27] When doped with Eu^{2+}, they show broad excitation bands in ultraviolet and blue regions, and a narrow FWHM (~ 50-60 nm) emission in the green region (500-560 nm).[14, 15, 27] These properties make Eu^{2+}-doped MGa_2S_4 very attractive as conversion phosphors for blue-emitting LEDs and backlight applications.

The optical properties of Eu^{2+}-doped $ZnGa_2S_4$ and $MgGa_2S_4$ are very close to each other.[14, 15] Recently, Joos et al. have proved by electron microscopy-based local analysis that the green emission observed for Eu^{2+}-doped $ZnGa_2S_4$ is actually not coming from Eu^{2+} in $ZnGa_2S_4$, but from a small fraction of $EuGa_2S_4$.[28] Moreover, they have found by XRD and EXAFS analysis that if any Eu is incorporated into the $ZnGa_2S_4$ host-lattice, it will occupy octahedral voids, which will induce the removal of neighboring Zn ions to compensate excess positive charges. Although such study was not performed on Eu^{2+}-doped $MgGa_2S_4$, in reason of the similarity of $ZnGa_2S_4$ and $MgGa_2S_4$ in terms of structural and optical properties, it is likely that a similar phenomenon is occurring. Thus, the reported values for Eu^{2+} in $ZnGa_2S_4$ and $MgGa_2S_4$ are considered doubtful, and in the following, we will focus more on M= Ca, Sr and Ba.

The FHWM is 50 nm for M = Ca and Sr,[9, 16] which is remarkably small for such Eu^{2+}-doped phosphors considering that both Ca- and Sr-thiogallates have 3 eightfold-coordinated M sites, where one may expect an overlapping of several Eu^{2+} emission bands. It may be due to a preferential Eu^{2+} occupation among the 3 available M^{2+} sites, as it was the case for $CaAl_2S_4$ or Sr_2SiS_4.[29, 30] In the case of Eu^{2+}-doped $BaGa_2S_4$, the FWHM is 60 nm,[10] which may be related to the fact that Eu^{2+} can occupy both Ba sites and/or to the larger Stokes shift, which is 0.5 eV for M=Ba versus 0.26 eV for M=Ca and Sr.

The values reported for the band-gap can differ, depending on how the band-gap is defined, namely as the fundamental absorption onset, the peak of exciton creation or the mobility band gap. Thus, different values of the band-gap for M= Ca, Sr and Ba have been reported.[9, 10, 12, 31, 32, 33] Until now, the best and most accurate determination of E^{ex}, which is related to the band

gap, for Eu^{2+}-doped $CaGa_2S_4$ has probably been determined by high-resolution time resolved spectroscopy using synchrotron radiation.[34] From the excitation spectrum of host emission, a clear band peaking at 275 nm (4.52 eV) is observed. This value is also the value that can be determined for Eu^{2+}-doped $CaGa_2S_4$ from the excitation spectrum of Eu^{2+} emission by Nazarov et al.[27] Due to this similarity and the fact that Nazarov et al. have also measured under the same conditions the excitation spectrum of Eu^{2+} emission in $BaGa_2S_4$ and $SrGa_2S_4$, we have decided to report the values based on the reference [27]. Thus, E^{ex} is 4.52, 4.89 and 4.07 eV for M= Ca, Sr and Ba, respectively.

$T_{50\%}$ is 400 K for M=Ca,[9] ~475 K for M=Sr,[16] and 420 K for M=Ba.[10] Thus, Eu^{2+}-doped $SrGa_2S_4$ is significantly different compared to the others in terms of thermal quenching temperature. The difference with Eu^{2+}-doped $CaGa_2S_4$ is more particularly intriguing since both have the same structure. The Eu concentration also has an impact on the thermal quenching properties of Eu^{2+}-doped $SrGa_2S_4$.[17] Values $T_{50\%}$ of 475, 460, 445, 435 and 385 K are reported for 1, 3, 7, 15 and 30% of Eu, respectively. Namely, the thermal quenching of Eu^{2+} emission in $SrGa_2S_4$ becomes stronger with increasing Eu concentration.

The quenching of 5d-4f emission in Eu^{2+} was generally explained by the Blasse-Bril model, which attributes the quenching to a large displacement between the ground and excited states of Eu^{2+} in the configuration coordinate diagram.[35] Such displacement is directly related to ΔS. In this model, ΔS should scale with the size of site occupied by Eu^{2+} and there should be a relationship between ΔS and $T_{50\%}$. However, for Eu^{2+}-doped $CaGa_2S_4$ and $SrGa_2S_4$, it is clearly not the case: while ΔS is 0.26 eV for both compounds, $T_{50\%}$ is different. We propose that the thermal ionization model may give a better explanation to the difference in the thermal quenching between Eu^{2+}-doped $CaGa_2S_4$ and $SrGa_2S_4$.[20]

III The vacuum referred binding energy schemes

In order to understand the thermal quenching differences between the iso-structural compounds $CaGa_2S_4$ and $SrGa_2S_4$, we have constructed the VRBE schemes to determine the energy difference between the Eu^{2+} 5d excited state level and the CB bottom (E_{dC}), which is related to the effective barrier energy for thermal quenching.[20]

The VRBE schemes as constructed for divalent and trivalent lanthanides in $CaGa_2S_4$ and $SrGa_2S_4$ are shown in Figure 1. The details concerning the physical background of the employed chemical shift method can be found in [36-38]. The model allows the prediction of the binding energy in the ground and excited states of each lanthanide ion in bi- and tri-valent

states. Thus, the determination by spectroscopy of a few parameters (in eV), i.e. the redshift D, the charge transfer energy ($E^{CT}(n,3+)$) from the valence band to the lowest binding energy in the ground state of Ln^{3+}, the energy needed for host exciton creation E^{ex}, and the Coulomb repulsion energy for $Eu^{2+/3+}$ (U(6)), defined as the energy difference between the ground state energy of Eu^{2+} and that of Eu^{3+}, is enough for the construction of the VRBE scheme of the lanthanide ions for a given material.

In practice, U(6) is empirically related to the centroid shift of the Ce^{3+} ion in the investigated material $\varepsilon_c(1,3+)$, namely the difference between the average energy of the 5d-levels in gaseous Ce^{3+}, which is 6.35 eV, and the average energy of the five 5d-levels of Ce^{3+} in the material $E^C(1,3+)$. Typically, $\varepsilon_c(1,3+)$, can be determined more accurately than U(6), as Ce^{3+} has only one electron in the 4f-shell leading to the most simple 4f-5d excitation spectra and the energies of the 4f-5d transitions are the lowest amongst all trivalent lanthanides, which can be conveniently studied in the UV-VIS part of the spectrum:[36-38]

$$\varepsilon_c(1,3+) = 6.35 - E^C(1,3+) \qquad (Eq.\ 1)$$

$$U(6) = 5.44 + 2.834\ exp(-\varepsilon_c(1,3+)/2.2) \qquad (Eq.\ 2)$$

From U(6), the absolute position of the lowest binding energy in the ground state of Eu^{2+}, $E_{4f}(7,2+)$, is determined by the equation:[36]

$$E_{4f}(7,2+) = -24.92 + (18.05-U(6))/(0.777-0.0353U(6)) \qquad (Eq.\ 3)$$

Moreover, the position of the lowest binding energy in the ground state of Eu^{3+}, $E_{4f}(6,3+)$ can be positioned via the relation:[36]

$$E_{4f}(6,3+) = E_{4f}(7,2+) - U(6) \qquad (Eq.\ 4)$$

The E_{4f} and the E_{5d} energy levels of bivalent and trivalent Eu are linked by the equation:[38]

$$E_{5d}(7,2+) = E_{4f}(7,2+) + (E_{fd}(7,2+,free) - D(2+)) \qquad (Eq.\ 5)$$

$$E_{5d}(6,3+) = E_{4f}(6,3+) + (E_{fd}(6,3+,free) - D(3+)) \qquad (Eq.\ 6)$$

with $E_{fd}(7,2+,free)$ and D(2+) the energy of the first lowest energy of 4f-5d transition in quasi-free state, which corresponds to 4.22 eV,[38] and the redshift of Eu^{2+}, respectively, and $E_{fd}(6,3+,free)$, which corresponds to 10.5 eV,[38] and D(3+) those of Eu^{3+}. Both D(2+) and D(3+) are usually not simultaneously experimentally determinable for a given sample, however one can be obtained from the other from the relationship:[37]

$$D(2+) = 0.64\ D(3+) - 0.233 \qquad (Eq.\ 7)$$

From the knowledge of the different energy levels of Eu^{2+} and Eu^{3+}, the energy levels of the other lanthanides are known, as they are shifted to each other by constants rather invariant of the type of compounds, which forms the well-established double zigzag curves.[39]

The top of the valence band, E_V, is calculated by the relation between $E^{CT}(6,3+)$ and the $E_{4f}(7,2+)$ level of the investigated lanthanide in the trivalent and divalent states, respectively:[38]

$$E_V = E_{4f}(7,2+) - E^{CT}(6,3+) \qquad (Eq.\ 8)$$

From the position of E_V, the exciton creation energy E^{ex}, and the electron-hole binding energy E_{eh} in the exciton state, the VRBE of the electron in the exciton state E_X and at the bottom of the conduction band E_C, are found:

$$E_X = E_V + E^{ex} \qquad (Eq.\ 9)$$

$$E_C = E_X + E_{eh} \qquad (Eq.\ 10)$$

For wide band-gap ionic compounds, E_{eh} is estimated at 8% of the band-gap energy. It appears that this percentage lowers when moving to smaller band-gap, namely more covalent, compounds, such as $CaGa_2S_4$ and $SrGa_2S_4$. Thus, as approximation, we estimated that the exciton binding energy is ~4-5% of the band-gap, so about ~ 0.2 eV.[40]

Finally, E_{dC} is determined by the equation:[41]

$$E_{dC} = E_{vc} - E^{CT}(6,3+) - E_{fd}(7,2+) \qquad (Eq.\ 11)$$

with E_{vc} the energy difference between E_V and E_C, and $E_{fd}(7,2+)$ the energy difference between $E_{5d}(7,2+)$ and $E_{4f}(7,2+)$.

Table 2 summarizes the experimental input data collected from the cited literature used to construct the VRBE schemes shown in Figure 1, and the model output data. We selected data pertaining to compounds with the lowest Eu^{2+} concentration and if available measured at low temperature, in order to prevent a possible influence from concentration or thermal quenching. U(6) was found to be 6.25 and 6.30 eV for $CaGa_2S_4$ and $SrGa_2S_4$, respectively.[38] For D(2+), the values of 1.86 and 1.64 eV for $CaGa_2S_4$ and $SrGa_2S_4$, respectively, were chosen as they correspond to the lowest Eu^{2+} concentration reported, in the best of our knowledge.[9, 34] For E^{ex}, 4.52 and 4.89 eV for $CaGa_2S_4$ and $SrGa_2S_4$, respectively, were taken, as discussed previously in the section 2.[27, 34] For E^{CT}, Eu^{3+} being not stable in MGa_2S_4, we used the E^{CT} of Er^{3+} for $SrGa_2S_4$,[42] and Tm^{3+} for $CaGa_2S_4$,[43, 44] and then removed a constant (2.58 eV in the case of Er^{3+} and 1.72 eV in the case of Tm^{3+}) to obtain $E^{CT}(6,3+)$.[37] For Tm^{3+}, we have done the average of 2 recent reported values. It may be noted that it has been recently found that a highly deformed first coordination shell is obtained for Ce^{3+}-doped $SrGa_2S_4$ It is most likely that such deformation should also occur for other trivalent ions in $SrGa_2S_4$, such as Tm^{3+} and Er^{3+}.[45] Moreover, the absolute values of energies given by the VRBE schemes can differ as much as ±0.5 eV, a detailed evaluation of possible contributions to errors in positioning the energy levels being given by Joos *et al.*.[43] However, such errors are highly systematic, and it

should not affect the qualitative fact that E_{dC} of $SrGa_2S_4$ (0.97 eV) is found significantly larger compared to that of E_{dC} of $CaGa_2S_4$ (0.75 eV), which is in agreement with E_{dC} determined from other reported VRBE diagrams of $SrGa_2S_4$ (0.67 eV) [45] and $CaGa_2S_4$ (0.19 eV).[43]

IV Discussion

Literature has shown experimentally that $T_{50\%}$, for the same Eu concentration, significantly differs: 400 K for 2% Eu^{2+}:$CaGa_2S_4$ and 475 K for 1% Eu^{2+}:$SrGa_2S_4$.[9, 16] The VRBE diagram in Figure 1 shows that E_{dC} is 0.75 and 0.97 eV for $CaGa_2S_4$ and $SrGa_2S_4$, respectively. These energies correspond in a qualitative way with differences in $T_{50\%}$ values, since, in the model of thermal quenching by thermal ionization, the rate of electron escape increases with increasing the temperature and with decreasing E_{dC}.[20] Moreover, they can explain the fact that the thermal quenching of Eu^{2+} emission in $SrGa_2S_4$ is larger for higher Eu concentration. Indeed, the unoccupied Eu 5d states form a rather localized band near the bottom of the conduction band. With increasing Eu concentration, possibility of local Eu clustering increases and the interactions among Eu 5d – Eu 5d orbitals become stronger. They cause delocalization of the Eu 5d band and decreasing of the life time of the excited electrons at the Eu 5d states, which caused quenching of photo emission.

E_{dC} is determined by the values of $E_{4f}(7,2+)$, $E_{5d}(7,2+)$, E^{CT} , E_V and E_C. E_V of $CaGa_2S_4$ (-5.32 eV) is slightly lower than E_C of $SrGa_2S_4$ (-5.27 eV). E^{CT} of $CaGa_2S_4$ (1.61 eV) is slightly higher than that of $SrGa_2S_4$ (1.54 eV), as expected for Ca^{2+} being smaller than Sr^{2+}.[46, 47] The difference between $E_{4f}(7,2+)$ and $E_{5d}(7,2+)$ of $CaGa_2S_4$ (2.36 eV) is smaller than that of $SrGa_2S_4$ (2.58 eV), which it is also expected due to the larger crystal field splitting for Ca^{2+} (2.09 eV) compared to Sr^{2+} (2.0 eV).[27] However, E_C for $CaGa_2S_4$ is 0.42 eV lower than that of $SrGa_2S_4$, which contradicts expectation. Indeed, based on an extensive overview of thermal quenching of Eu^{2+} emission in different compounds, two different types of compounds were discriminated:[20]

1) In type I compounds, E_C is mainly composed of orbitals of cations that are being substituted by Eu^{2+}, e.g. MF_2 (M = Ca, Sr, Ba). The quenching temperature tends to increase with smaller size of the cation.

2) In type II compounds, E_C is composed of orbitals of cations other than the one replaced by Eu^{2+}. This is the situation expected in alkaline earth silicates $MSiO_3$ (M= Ca, Sr, Ba) and the thiogallates MGa_2S_4 (M = Ca, Sr) reported in this publication. E_C does not significantly

depend on the type of M, thus E_C is expected to be about the same for Eu^{2+}:$CaGa_2S_4$ and Eu^{2+}:$SrGa_2S_4$ in first approximation, which is clearly not the case.

To clarify the nature of the contribution of the different elements to the electronic properties of $CaGa_2S_4$ and $SrGa_2S_4$, electronic structure calculations were performed using the first-principles code VASP (Vienna *Ab initio* Simulation Program),[48, 49] which employs the density functional theory (DFT)[50, 51] within the Projector Augmented-Wave (PAW)[52, 53] method that belongs to Generalized Gradient Approximation (GGA) by Perdew-Burke-Ernzerhof (PBE).[54] The cut-off energy of the wave functions is 500 eV and that of the augmentation wave functions 700 eV. The electronic wave functions were sampled on dense grids in the Brillouin zone (BZ) of crystals using the Monkhorst and Pack method.[55] Tests showed that the present settings produced reliable results with good convergence within 1 meV/atom. The calculated total and partial density of states (DOS) curves are shown in Figure 2. The lower part of the valence bands (from -6 to -4 eV), is dominated by S 3p and Ga 4s, while the upper part (from -4 to 0 eV) by S 3p and Ga 4p. The lower part of the conduction bands (from 3 to 4.5 eV) are dominated by Ga 4s states. The calculated band gap is about 3.0 eV, which is lower than the experimental values. This is not unusual since the DFT generally underestimates band gaps of semiconducting/insulating compounds.[56] The Fermi level is set to be at the top of the valence band. The contribution of the Ca 3d/Sr 4d states are more dominant in the upper part of the conduction bands (from 4.5 eV). Namely, the hybridization between the S 3p and Ga 4p determines the band structure near the Fermi level due to the covalent nature between Ga and S. Therefore, the overall electronic properties of the $CaGa_2S_4$ and $SrGa_2S_4$ crystals are largely determined by the Ga-S framework. In other words, they are not related to the states of the alkaline earth cation. So, in order to understand the origin of the low lying conduction band in $CaGa_2S_4$ versus $SrGa_2S_4$, one has to understand why the Ga 4s states have low VRBE.

In both $CaGa_2S_4$ and $SrGa_2S_4$, Ga occupy 2 sites that are in the center of a sulphur tetrahedron. In order to investigate the differences, the Ga-S distances determined by Rietveld refinement from the investigation of Nazarov et al. are reported in Table 3. In $CaGa_2S_4$, the average bond length of the four Ga-S bonds is 224.8 pm with a bond length variation of at most 2.3 pm for Ga1 and 225.2 pm with a variation of 4.2 pm for Ga2, suggesting that the tetrahedral coordination is reasonably regular. In contrast, for $SrGa_2S_4$, the average Ga-S bond length is 226.6 pm with a bond length variation of 24 pm for the Ga1 site, and 228.1 pm with a variation of 10 pm for the Ga2 site. So, the tetrahedrons are quite distorted, with one of the Ga-S2 bonds being much shorter compared to the three others.

Interestingly, while the average Ga-S bond lengths for $SrGa_2S_4$ are larger compared to those for $CaGa_2S_4$, which is expected as the size of Sr^{2+} is larger than that of Ca^{2+}, the shortest Ga-S bond length of $SrGa_2S_4$ is smaller than that of $CaGa_2S_4$. This suggests that the thermal quenching of Eu^{2+} emission is controlled by local environment and not the average one. The VRBE of the electron in the 4s-orbital dominated CB-bottom is determined by the Coulomb bonding to the positive Ga ion and the Coulomb repulsion from the negative sulphur ligands. Apparently the short Ga-S bond in $SrGa_2S_4$ leads to larger repulsion and likewise less negative VRBE at the conduction band bottom. This translates to an increase of E_{dC} with corresponding higher quenching temperature of the Eu^{2+} 5d-4f emission for Eu^{2+}-doped $SrGa_2S_4$ compared to Eu^{2+}-doped $CaGa_2S_4$. A change of the shortest Ga-S bond length, for instance by the presence of defects present in the material and/or a preferential distribution of Eu in $SrGa_2S_4$, may strongly affect the quenching temperature. It also suggests that manipulating the Ga-S distances in a desired direction by controlled chemical substitution may effectively improve the thermal quenching behavior in such phosphors.

Conclusions

The VRBE schemes were constructed for $CaGa_2S_4$ and $SrGa_2S_4$ based on the literature data. The 5d energy of Eu^{2+} was found at 0.75 and 0.97 eV below the bottom of the conduction band for $CaGa_2S_4$ and $SrGa_2S_4$, respectively. The values correspond well with the higher thermal quenching temperatures reported for Eu^{2+}-doped $SrGa_2S_4$ ($T_{50\%}$ = ~475 K) as compared to Eu^{2+}-doped $CaGa_2S_4$ ($T_{50\%}$ = 400 K). As the Eu^{2+} 5d level has been found at similar energies in both $CaGa_2S_4$ and $SrGa_2S_4$, so the main reason for the variation in $T_{50\%}$ is the difference in the position of the conduction band bottom. Theoretical studies have shown that the overall electronic properties of the $CaGa_2S_4$ and $SrGa_2S_4$ crystals are largely determined by the Ga-S framework. The structural data show that the GaS_4 tetrahedrons are distorted in $SrGa_2S_4$ while these are quite regular in $CaGa_2S_4$. As a consequence of a shorter Ga-S bond length in $SrGa_2S_4$ compared to $CaGa_2S_4$, the repulsion between electrons on Ga and S is stronger for $SrGa_2S_4$ versus $CaGa_2S_4$, resulting in a higher energy position of the conduction band bottom and consequently a higher $T_{50\%}$ for Eu^{2+}-doped $SrGa_2S_4$ than for iso-structural Eu^{2+}-doped $CaGa_2S_4$.

Acknowledgements

The authors are grateful to Dr. J. Joos and Prof. P. Smet of Ghent University for fruitful discussions and feedbacks.

References

[1]R.J. Xie, N. Hirosaki, Sci. Technol. Adv. Mater. 8 (2007) 588.

[2]X.H. He, L. N. Lian, J.H. Sun, M.Y. Guan, J. Mater. Sci. 44 (2009) 4763.

[3]H.A. Höppe, Angew. Chem. Int. Ed. 48 (2009) 3572.

[4]P.F. Smet, I. Moreels, Z. Hens, D. Poelman, Materials 3 (2010) 2834.

[5]C. Che, R.S. Liu, J. Phys. Chem. Lett. 2 (2011) 1268.

[5]R.-J Xie, H.T. Hintzen, J. Am. Ceram. Soc. 96 (2013) 665.

[6]M. Sato, S.W. Kim, Y. Shimomura, T. Hasegawa, K. Toda, G. Adachi, Handbook on the Physics and Chemistry of Rare Earths 49 (2016) 1.

[7]U. Kaufmann, M. Kunzer, K. Köhler, H. Obloh, W. Pletschen, P. Schlotter, J. Wagner, A. Ellens, W. Rossnes, M. Kobuschm, Phys. Stat. Sol. (a) 192 (2002) 246.

[8]T.E. Peters, J.A. Baglio, J. Electrochem. Soc. 119 (1972) 230.

[9]C. Chartier, C. Barthou, P. Benalloul, J.M. Frigerio, J. Lumin. 11 (2005) 147.

[10]R.B. Jabbarov, C. Chartier, B.G. Tagiev, O.B. Tagiev, N.N. Musayeva, C. Barthou, P. Benalloul, J. Phys. Chem. Solids 66 (2005) 1049.

[11]C. Guo, Q. Tang, D. Huang, C. Zhang, Q. Su, J. Phys. Chem. Solids 68 (2007) 217.

[12]H.S. Yoo, W.B. Im, S. Vaidyanathan, B.J. Park, D.Y. Jeon, J. Electrochem. Soc. 155 (2008) J66.

[13]M. Nazarov, B. Tsukerblat, D.Y. Noh, J. Phys. Chem. Solids 69 (2008) 2605.

[14]R. Yu, R. Luan, C. Wang, J. Chen, Z. Wang, B.K. Moon, J.H. Jeong, J. Electrochem. Soc. 159 (2012) J188.

[15]R. Yu, H.M. Noh, B.K. Moon, B.C. Choi, J.H. Jeong, K. Jang, S.S. Yi, J.K. Jang, J. Am. Ceram. Soc. 96 (2013) 1821.

[16]P. Benalloul, C. Barthou, C. Fouassier, A.N. Georgobiani, L.S. Lepnev, Y.N. Emirov, A.N. Gruzintsev, B.G. Tagiev, O.B. Tagiev, R.B. Jabbarov, J. Electrochem. Soc. 150 (2003) G62.

[17]J.J. Joos, K.W. Meert, A.B. Parmentier, D. Poelman, P.F. Smet, Opt. Mater. 34 (2012) 1902.

[18]M.R. Davolos, A. Garcia, C. Fouassier, P. Hagenmuller, J. Solid State Chem. 83 (1989) 316.

[19]H. Najafov, A. Kato, H. Toyota, K. Iwai, A. Bayramov, S. Iida, Jpn. J. Appl. Phys. 41 (2002) 1424.

[20]P. Dorenbos, J. Phys. Condens. Matter. 20 (2005) 8103.

[21]J. Ueda, T. Shinoda, S. Tanabe, Opt. Mater. 41 (2015) 84.

[22]E. van der Kolk, P. Dorenbos, J.T.M. de Haas, C.W.E. van Eijk, Phys. Rev. B 71 (2005) 045121.

[23]T. Shalapska, G. Stryganyuk, A Gektin, P. Demchenko, A Voloshinovskii, P. Dorenbos, J. Phys. Condens. Matter. 22 (2010) 485503.
[24]R.L. Nyenge, H.C. Swart, O.M. Ntwaeaborwa, Opt. Mater. 40 (2015) 68.
[25]G.B. Carpenter, P. Wu, Y.M. Gao, A. Wold, Mater. Res. Bull. 24 (1989) 1077.
[26]C. Romers, B.A. Blaisse, D.J.W. IJdo, Acta Cryst. 23 (1967) 634.
[27]M. Nazarov, D.Y. Noh, H. Kim, Mater. Chem. Phys. 107 (2008) 456.
[28]J.J. Joos, K. Korthout, S. Nikitenko, D. Poelman, P.F. Smet, Opt. Mater. Express 3, (2013) 1338.
[29]J.E. van Haecke, P.F. Smet, D. Poelman, J. Lumin. 126 (2007) 508.
[30]A.B. Parmentier, P.F. Smet, D. Poelman, Materials 6 (2013) 3663.
[31]C. Hidaka, T. Takizawa, J. Cryst. Growth 237-239 (2002) 2009.
[32]T. Takizawa, C. Hidaka, J. Phys. Chem. 69 (2008) 347.
[33]Z. Xinmin, W. Hao, Z. Heping, S. Qiang, J. Rare Earths 25 (2007) 701.
[34]A. Bessière, P. Dorenbos, C.W.E va Eijk, E. Yamagishi, C. Hidaka, T. Takizawa, J. Electrochem. Soc. 151 (2004) H254.
[35]G. Blasse, A. Bril, Phil. Tech. Rev. 31 (1970) 304.
[36]P. Dorenbos, Phys. Rev. B 85 (2012) 165107.
[37]P. Dorenbos, ECS J. Solid State Sci. Technol. 2 (2013) R3001.
[38]P. Dorenbos, J. Lumin. 135 (2013) 93.
[39]J. Sugar, J. Reader, J. Chem. Phys.59 (1973) 2083.
[40]P. Dorenbos, J. Lumin. 111 (2005) 89.
[41]P. Dorenbos, J. Phys.: Condens. Matter 15 (2005) 8417.
[42]A. Garcia, C. Fouassier, P. Dougier, J. Electrochem. Soc. 129 (1982) 2063.
[43]J.J. Joos, D. Poelman, P.F. Smet, Phys. Chem. Chem. Phys. 17 (2015) 19058.
[44]A. Garcia, F. Guillen, C. Fouassier, J. Lumin. 33 (1985) 15.
[45]J.J. Joos, D. Poelman, P.F. Smet, Opt. Mater. in press (2016).
[46]H.E. Hoefdraad, J. Solid State Chem. 15 (1975) 175.
[47]R.D. Shannon, Acta Cryst. A32 (1976) 751.
[48]G. Kresse, J. Hafner, Phys. Rev. B 49 (1994) 14251.
[49]G. Kresse, J. Furthműller, J. Comput. Mater. Sci. 6 (1996) 15.
[50]P. Hohenberg, W. Kohn, Phys. Rev. 136 (1964) B864.
[51]W. Kohn, L. J. Sham, Phys. Rev. 140 (1965) A1133.
[52]P.E. Blöchl, Phys. Rev. B 50 (1994) 17953.
[53]G. Kresse, J. Joubert, Phys. Rev. B 59 (1999) 1758.

[54]J. P. Perdew, K. Burke, M. Ernzerhof, Phys. Rev. Lett. 77 (1996) 3865.

[55]H. J. Monkhorst, J. D. Pack, Phys. Rev. B 13 (1976) 5188.

[56]R. O. Jones, Rev. Mod. Phys. 87 (2015) 897.

Captions

Table 1. Comparison of the structural and optical properties of MGa_2S_4 (M=Zn, Mg, Ca, Sr or Ba) doped with a comparable concentration of Eu^{2+} (Δ: 5-7 Eu%, #: 0.1-2%Eu) – *The values indicated may be actually related to $EuGa_2S_4$.

Table 2. Experimental input data used to construct the VRBE schemes for the divalent and trivalent lanthanides doped in $CaGa_2S_4$ (a) and $SrGa_2S_4$ (b), shown on Figure 1, and the model output data to construct the VRBE scheme for MGa_2S_4 (M=Ca or Sr). All energies are in eV. The experimental input data are indicated in italic.

Figure 1. VRBE schemes for the divalent and trivalent lanthanides doped in $CaGa_2S_4$ (a) and $SrGa_2S_4$ (b).

Figure 2. PBE calculations of the total density of states (DOS) of and partial DOS of the metallic atoms/ions in $CaGa_2S_4$ and $SrGa_2S_4$ crystals. The pDOS of S atoms/ions are not included.

Table 3. Ga-S distances in Eu^{2+}-doped $CaGa_2S_4$ and Eu^{2+}-doped $SrGa_2S_4$.

Parameters	Zn	Mg	Ca	Sr	Ba
Crystal system	Tetragonal [25]	Monoclinic [26]	Orthorhombic [27]	Orthorhombic [27]	Cubic [27]
Space group	I-42m (121) [25]	C12/c1 (15) [26]	Fddd (70) [27]	Fddd (70) [27]	Pa-3 (205) [27]
α/β/γ (°)	90/90/90 [25]	90/108,8/90 [26]	90/90/90 [27]	90/90/90 [27]	90/90/90 [27]
a (Å)	5,297 [25]	12,74 [26]	12,21 [27]	12,21 [27]	12,68 [27]
b (Å)	5,297 [25]	22,54 [26]	20,09 [27]	20,51 [27]	12,68 [27]
c (Å)	10,36 [25]	6,43 [26]	20,12 [27]	20,86 [27]	12,68 [27]
V ($Å^3$)	290,8 [25]	174,79 [26]	4904,8 [27]	5224,87 [27]	2041,1 [27]
M site number	1 [25]	3 [26]	3 [27]	3 [27]	2 [27]
CN of each M site	4 [25]	6/6/6 [26]	8/8/8 [27]	8/8/8 [27]	6/12 [27]
Ga site number	2 [25]	3 [26]	2 [27]	2 [27]	1 [27]
CN of each Ga site	4/4 [25]	4/4/4 [26]	4/4 [27]	4/4 [27]	4 [27]
E^{ex} (eV)	4,44 [14]	4,14 [15]	4,52 [27]	4,89 [27]	4,07 [27]
E_{df} (eV – nm) $^{\Delta}$	2,30 – 540 [14]*	2,31 – 538 [15]*	2,23 – 558 [27]	2,32 – 535 [27]	2,46 – 504 [27]
E_0 (eV – nm) $^{\Delta}$	2,41 – 515 [14]*	2,42 – 514 [15]*	2,35 – 529 [27]	2,44 – 508 [27]	2,68 – 464 [27]
E_{fd} (eV – nm) $^{\Delta}$	2,53 – 490 [14]*	2,53 – 490 [15]*	2,48 – 500 [27]	2,58 – 482 [27]	2,93 – 424 [27]
ΔS (eV) $^{\Delta}$	0,22 [14]*	0,23 [15]*	0,26 [27]	0,26 [27]	0,5 [27]
D (eV) $^{\Delta}$	1,69 [14]*	1,66 [15]*	1,71 [27]	1,62 [27]	1,3 [27]
FWHM (RT/450K) (nm)	45/49 [14]$^{\Delta}$*	49/59 [15]$^{\Delta}$*	50/58 [16]$^{\#}$	50/59 [9]$^{\#}$	60/70 [10]$^{\#}$
I_{420K}/I_{RT}	0,42 [14]$^{\Delta}$*	0,44 [15]$^{\Delta}$*	0,36 [16]$^{\#}$	0,66 [9]$^{\#}$	0,5 [10]$^{\#}$
$T_{50\%}$ (K)	402 [14]$^{\Delta}$*	407 [15]$^{\Delta}$*	400 [16]$^{\#}$	475 [9]$^{\#}$	420 [10]$^{\#}$

Table 1. Comparison of the structural and optical properties of MGa_2S_4 (M=Zn, Mg, Ca, Sr or Ba) doped with a comparable concentration of Eu^{2+} (Δ: 5-7 Eu%, #: 0.1-2%Eu) – *The values indicated may be actually related to $EuGa_2S_4$.

Parameters	Ca	Sr
U(6)	*6,25 [38]*	*6,30 [38]*
$E_{4f}(7,2+)$	-3,71	-3,73
$E_{4f}(6,3+)$	-9,96	-10,03
D(2+)	*1,86 [34]*	*1,64 [9]*
D(3+)	3,27	2,93
$E_{5d}(7,2+)$	-1,35	-1,15
$E_{5d}(6,3+)$	-2,73	-2,46
E^{CT}	*3.29 – 3,37 (Tm^{3+}) [43, 44]*	*4,12 (Er^{3+}) [42]*
E^{CT} (Eu^{3+})	1,61	1,54
E_V	-5,32	-5,27
E^{ex}	*4,52 [34]*	*4,89 [27]*
E_X	-0,80	-0,38
E_C	-0,60	-0,18
ΔE_{dC}	0,75	0,97

Table 2. Experimental input data used to construct the VRBE schemes for the divalent and trivalent lanthanides doped in $CaGa_2S_4$ (a) and $SrGa_2S_4$ (b), shown on Figure 1, and the model output data to construct the VRBE scheme for MGa_2S_4 (M=Ca or Sr). All energies are in eV. The experimental input data are indicated in italic.

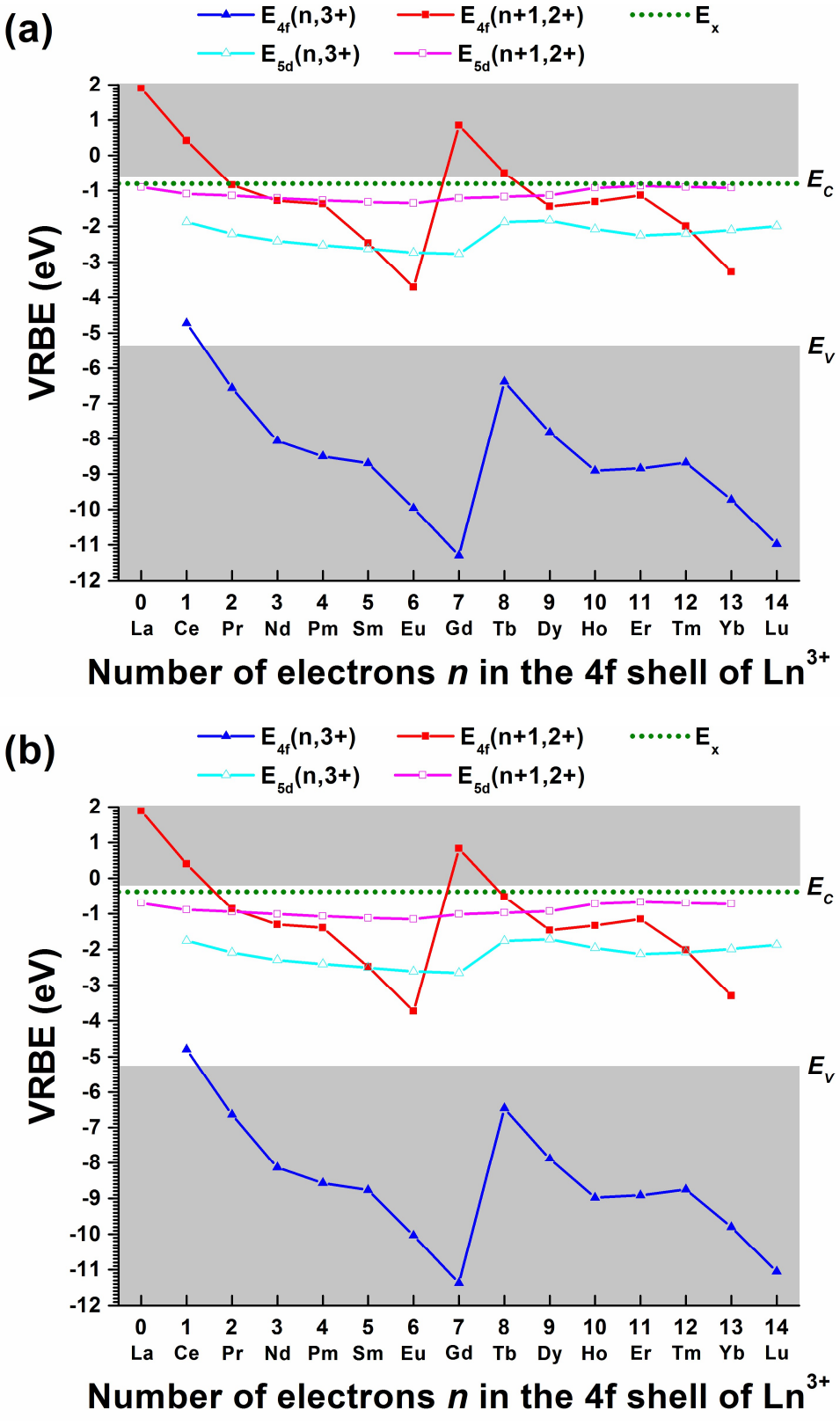

Figure 1. VRBE schemes for the divalent and trivalent lanthanides doped in $CaGa_2S_4$ (a) and $SrGa_2S_4$ (b).

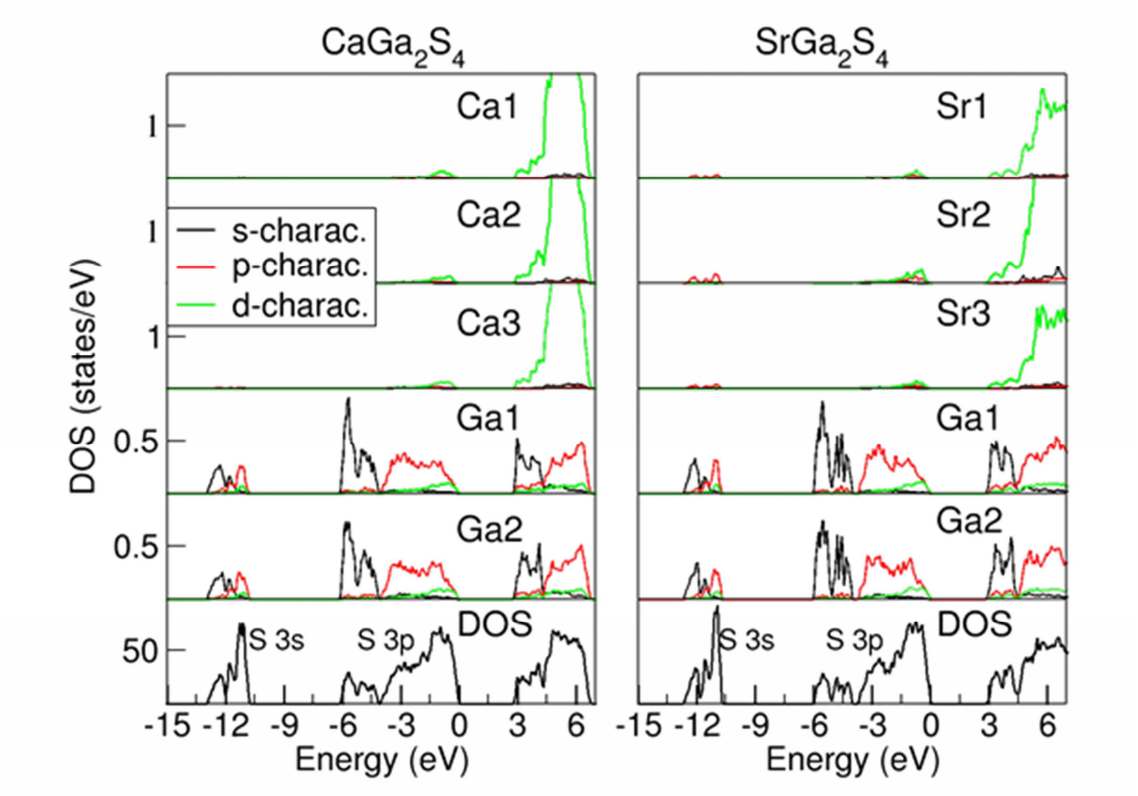

Figure 2. PBE calculations of the total density of states (DOS) of and partial DOS of the metallic atoms/ions in $CaGa_2S_4$ and $SrGa_2S_4$ crystals. The pDOS of S atoms/ions are not included.

Ga-S	$CaGa_2S_4$ (pm)	$SrGa_2S_4$ (pm)
Ga1-S2	224,2	203,1
Ga1-S2	225,7	242,9
Ga1-S3	227,0	230,1
Ga1-S4	222,5	230,1
Average Ga1-S	224,9 ± 2,4	226,6 ± 23,5
Ga2-S1	226,9	237,5
Ga2-S1	225,7	227,5
Ga2-S3	221,0	218,4
Ga2-S4	227,2	229,0
Average Ga2-S	225,2 ± 4,2	228,1 ± 9,7

Table 3. Ga-S distances in Eu^{2+}-doped $CaGa_2S_4$ and Eu^{2+}-doped $SrGa_2S_4$.